Human Reproduction, Vol.36, No.10, pp. 2720–2731, 2021
Advance Access Publication on August 7, 2021 doi:10.1093/humrep/deab186

human reproduction

ORIGINAL ARTICLE *Reproductive biology*

Three-dimensional microengineered vascularised endometrium-on-a-chip

Jungho Ahn[1,2], Min-Ji Yoon[3], Seon-Hwa Hong[4], Hwijae Cha[3], Danbi Lee[3], Hwa Seon Koo[4], Ji-Eun Ko[4], Jungseub Lee[5], Soojung Oh[6], Noo Li Jeon[5], and Youn-Jung Kang [1,3,4,*]

[1]Department of Biochemistry, Research Institute for Basic Medical Science, School of Medicine, CHA University, Seongnam-si, Gyeonggi-do, Republic of Korea [2]Research Competency Milestones Program of School of Medicine, CHA University, Seongnam-si, Gyeonggi-do, Republic of Korea [3]Department of Biomedical Science, School of Life Science, CHA University, Seongnam-si, Gyeonggi-do, Republic of Korea [4]CHA Fertility Center Bundang, Seongnam-si, Gyeonggi-do, Republic of Korea [5]Department of Mechanical and Aerospace Engineering, Seoul National University, Seoul-si, Republic of Korea [6]AMOREPACIFIC Research and Development Center, Yongin-si, Gyeonggi-do, Republic of Korea

*Correspondence address. Department of Biochemistry, Research Institute for Basic Medical Science, School of Medicine, CHA University, 335 Pangyo-ro, Bundang-gu, Seongnam-si, Gyeonggi-do, Republic of Korea. E-mail:yjkang@cha.ac.kr
https://orcid.org/0000-0002-0771-9515

Submitted on March 9, 2021; resubmitted on May 17, 2021; editorial decision on July 19, 2021

STUDY QUESTION: Can we reconstitute physiologically relevant 3-dimensional (3D) microengineered endometrium *in-vitro* model?

SUMMARY ANSWER: Our representative microengineered vascularised endometrium on-a-chip closely recapitulates the endometrial microenvironment that consists of three distinct layers including epithelial cells, stromal fibroblasts and endothelial cells in a 3D extracellular matrix in a spatiotemporal manner.

WHAT IS KNOWN ALREADY: Organ-on-a-chip, a multi-channel 3D microfluidic cell culture system, is widely used to investigate physiologically relevant responses of organ systems.

STUDY DESIGN, SIZE, DURATION: The device consists of five microchannels that are arrayed in parallel and partitioned by array of micropost. Two central channels are for 3D culture and morphogenesis of stromal fibroblast and endothelial cells. In addition, the outermost channel is for the culture of additional endometrial stromal fibroblasts that secrete biochemical cues to induce directional pro-angiogenic responses of endothelial cells. To seed endometrial epithelial cells, on Day 8, Ishikawa cells were introduced to one of the two medium channels to adhere on the gel surface. After that, the microengineered endometrium was cultured for an additional 5–6 days (total ~ 14 days) for the purpose of each experiment.

PARTICIPANTS/MATERIALS, SETTING, METHODS: Microfluidic 3D cultures were maintained in endothelial growth Medium 2 with or without oestradiol and progesterone. Some cultures additionally received exogenous pro-angiogenic factors. For the three distinct layers of microengineered endometrium-on-a-chip, the epithelium, stroma and blood vessel characteristics and drug response of each distinct layer in the microfluidic model were assessed morphologically and biochemically. The quantitative measurement of endometrial drug delivery was evaluated by the permeability coefficients.

MAIN RESULTS AND THE ROLE OF CHANCE: We established microengineered vascularised endometrium-on-chip, which consists of three distinct layers: epithelium, stroma and blood vessels. Our endometrium model faithfully recapitulates *in-vivo* endometrial vasculo-angiogenesis and hormonal responses displaying key features of the proliferative and secretory phases of the menstrual cycle. Furthermore, the effect of the emergency contraception drug levonorgestrel was evaluated in our model demonstrating increased endometrial permeability and blood vessel regression in a dose-dependent manner. We finally provided a proof of concept of the multi-layered endometrium model for embryo implantation, which aids a better understanding of the molecular and cellular mechanisms underlying this process.

LARGE SCALE DATA: N/A.

LIMITATIONS, REASONS FOR CAUTION: This report is largely an *in-vitro* study and it would be beneficial to validate our findings using human primary endometrial cells.

WIDER IMPLICATIONS OF THE FINDINGS: Our 3D microengineered vascularised endometrium-on-a-chip provides a new *in-vitro* approach to drug screening and drug discovery by mimicking the complicated behaviours of human endometrium. Thus, we suggest our

model as a tool for addressing critical challenges and unsolved problems in female diseases, such as endometriosis, uterine cancer and female infertility, in a personalised manner.

STUDY FUNDING/COMPETING INTEREST(S): This work is supported by funding from the National Research Foundation of Korea (NRF) grant funded by the Korea government (MSIT) to Y.J.K. (No. 2018R1C1B6003), to J.A. (No. 2020R1I1A1A01074136) and to H.S.K. (No. 2020R1C1C100787212). The authors report no conflicts of interest.

Key words: microfluidic / 3D culture / endometrium / endometrial angiogenesis / drug screening

Introduction

The endometrium is a highly specialised multi-layered organ in the human body that plays crucial roles in maintaining the patency of the uterine cavity (Taylor and Gomel, 2008). During the reproductive life, the human endometrium undergoes significant growth and regression in a cyclic manner and substantial but demarcated tissue breakdown in response to dynamic changes in the ovarian steroid hormones including oestrogen (E2) and progesterone (P4) (Reed and Carr, 2000). This multi-layered organ is comprised of a functionalis layer adjacent to the uterine lumen and a basalis layer next to the myometrium. These layers consist of several different cell types, including luminal and glandular epithelial cells, endometrial stromal cells, immune cells, and vascular cells which form the spiral arterioles (Kobayashi and Behringer, 2003; Roy and Matzuk, 2011; Hibaoui and Feki, 2020). The uterine cycle, which represents the preparation of the inner lining of the endometrium for implantation by an embryo and the shedding of the lining when implantation has failed, usually occurs over approximately 28 days (Reed and Carr, 2000). Following menstruation, during the proliferation phase, the endometrium becomes increasingly thick through the proliferation of epithelial, stromal and endothelial cells in response to elevating oestradiol levels. During the subsequent secretory phase, the corpus luteum produces progesterone, which plays a key role in endometrial vascular maturation and decidualisation, making the endometrium receptive to embryo implantation and supportive of early pregnancy (Brar *et al.*, 1997; Lim *et al.*, 1999). Although numerous animal studies have demonstrated the cyclic physiology of the endometrium, there remain substantial discrepancies among different species. Moreover, the lack of a physiologically relevant *in-vitro* model for the endometrium, with the given practical difficulties associated with access to primary cells and *in-vitro* maintenance of the multi-layered culture system, remains the main obstacle for research, suggesting the need for a more physiologically relevant model for the human endometrium (McGowen *et al.*, 2014; Catalini and Fedder, 2020).

Recently, microfluidic-based technology has attracted considerable interest in cell biology and medical research, due to its ability to better mimic the *in-vivo* cellular microenvironment compared to conventional macroscale cell culture platforms. With the significant advances in microfluidics and organs-on-chip research in recent years, several groups have reported the development of 3D microengineered platforms for recapitulating parts of the female reproductive system. These include the modelling of the human placental barrier using a compartmentalised multilayer microfluidic system by co-culturing a human trophoblast cell line and human umbilical vein endothelial cells (HUVECs) or human primary placental villous endothelial cells (Blundell *et al.*, 2016; Lee *et al.*, 2016). More recent works have produced organ-on-a-chip model that functionally recreates the entire 28-days of the menstrual cycle *in vitro*, where human and mouse cells from reproductive organs were grown in a network of interconnected microengineered units (Xiao *et al.*, 2017). In addition, it has been reported, that haemodynamic forces induce the secretion of specific endothelial cell-derived prostanoids which enhance endometrial perivascular decidualisation in a microfluidic multilayer perfusion culture (Gnecco *et al.*, 2019). Nonetheless, previous female reproductive systems have not been able to recapitulate the vascularised endometrial microenvironment, which is essential for understanding reproductive biology.

In this study, we have developed a microengineered vascularised endometrium-on-a-chip (MVEOC), which reconstitutes the physiologically relevant endometrial environment including three distinct layers of epithelium, stroma and blood vessels, and have demonstrated its appropriate responsiveness to pro-angiogenic factors and hormonal stimulation. Importantly, we have assessed the utility of MVEOC for testing the efficacy and safety of the clinically used emergency birth control drug levonorgestrel and to establish an advanced *in-vitro* model for embryo implantation. This approach provides an effective tool for drug screening and toxicity testing in the field of female reproduction and a tool for investigating the specific molecular mechanisms involved in reproductive biology, with potential applications in personalised medicine.

Materials and methods

Microfluidic device design and fabrication

A master with positive patterns of photoresist, SU-8 (MicroChem, Microchem Laboratory, Austin, TX, USA), on a silicon wafer was prepared using photolithography. The microfluidic devices were fabricated with polydimethylsiloxane (PDMS, Sylgard 184, Dow Corning, Midland, MI, USA) using soft lithography and replica moulding. The PDMS elastomer and curing agents were mixed at a ratio of 10:1 (w/w) and poured onto the master mould and cured for 1 h in an 80°C dry oven. After the cured PDMS was peeled off from the wafer, cell injection ports and reservoirs for culture media were punched out using a 1 mm and a 6 mm biopsy punch, respectively. The device was kept in an 80°C dry oven after plasma bonding for at least 48 h to make its surface hydrophobic and sterilised by UV irradiation before each experiment.

Cell culture

Human umbilical vein endothelial cells (HUVECs, Lonza) were cultured in endothelial growth medium 2 (EGM-2, Lonza) and passages 3–5 were used for the experiments. Endometrial epithelial cells (EECs:

Ishikawa) and endometrial stromal fibroblasts (ESFs: CRL-4003 cells), obtained from ATCC and the laboratory of Dr Haeng Seok Song, respectively, were maintained in DMEM/F12 medium (Gibco, Grand Island, NY, USA) supplemented with 10% fetal bovine serum (FBS; Gibco, Grand Island, NY, USA) and 1% penicillin–streptomycin (Gibco, Grand Island, NY, USA) as previously described (Kang *et al.*, 2015), and between passages 7 and 8 were used for all experiments. Red fluorescent protein (RFP)-labelled HUVECs (Angio-Proteomie; Boston, MA, USA) were procured at P3 and sub-cultured to produce P6 frozen stock. All cells were maintained in a humidified incubator at 37°C with 5% CO_2.

Hydrogel and cell loading

The device consisted of five microchannels arrayed in parallel and partitioned by an array of microposts (Fig. 1A). On Day 1, two central channels (Stroma-Angiogenic Sprout Channel: SC, and Vascular Network Channel: VC) were established for the development of a 3-dimensional (3D) culture system and observation of morphogenesis of HUVECs (endothelial cells; ECs). CRL-4003 (5×10^6 cells/ml) (endometrial stromal fibroblasts; ESFs)-embedded fibrin gel solution (2.5 mg/ml fibrinogen with 0.15 U/ml aprotinin) was loaded in the channel SC, and EC-embedded fibrin gel was loaded in the channel VC. In addition, the outermost channel (fibroblast channel, FC) was set for the culture of additional endometrial stromal fibroblasts (6×10^6 cells/ml) that might induce a pro-angiogenic response of ECs by secreting biochemical cues. After 3 min, the upper reservoirs of each device were filled with EGM-2 culture medium and aspirated gently from the lower reservoirs to wet the hydrophobic media channels, and media channels 1 and 2 (MC 1 and 2) were filled with EGM-2 media. The ECs in the VC could communicate via soluble secreted factors in a paracrine manner across the microfluidic channels. Subsequent cell cultures were conducted under static conditions. Following HUVEC elongation on Day 1, the formation of the vascular network and lumen structures was observed after 3–4 days. Further development of the angiogenic sprouts to the adjacent channel (SC) occurred from a densely interconnected microvascular network (VC) by Day 6. On Day 8, Ishikawa cells (EECs) were introduced at a concentration of 3×10^6 cells per ml to MC 1, which is next to the SC. The microfluidic device was then tilted by 90° and incubated for 30 min, allowing EECs to adhere to the surface of the gel. The device was incubated for 4–6 days to recreate the endometrial microenvironment. A schematic illustration of the cell loading and generation of the 3D endometrium model is shown in Fig. 1A and Supplementary Fig. S1.

Immunofluorescence staining and microscopy in a microfluidic platform

For immunofluorescence staining, cells in the device were fixed using 4% PFA for 15 min at room temperature (RT), permeabilised with Triton X-100 (0.15% v/v in PBS) for 15 min, and then blocked with bovine serum albumin (BSA 3% w/v in PBS) for 1 h at RT. Localisation studies were performed using monoclonal primary antibodies specific for human CD31 (Alexa Fluor647, 1:200, BioLegend, San Diego, CA, USA), Hoechst 33342 (1:1000, Molecular Probes, Eugene, OR, USA), anti-epithelial cell adhesion molecule EpCAM, CD326 (AlexaFluor 594, 1:200, BioLegend) and AlexaFluor 488 conjugated phalloidin (1:400, Molecular Probes), and further incubated with anti-rabbit IgG fluorescence (Invitrogen, Carlsbad, CA, USA) or anti-mouse IgG fluorescence (Invitrogen) as appropriate, all at 1:400 for 1 h. Images were captured using a confocal microscope (Nikon Ti2-E inverted microscope) and processed using Zen software (ZEISS, Jena, Germany).

Measurement of endometrium permeability in microfluidic platform

Diffusion of FITC-dextran (1 mg/ml in PBS) from endometrial epithelial cells (Ishikawa cell line) was imaged every 10 s to calculate the endometrium permeability coefficient. The permeability coefficient P was calculated based on a previously described equation (Ahn *et al.*, 2018).

$$P = \frac{I}{I_W} \times \frac{dI/dt}{I_j}$$

Here, I_W is the length of the endometrial wall border between the peri-endometrium and inner endometrium region, I_j is the mean intensity in the inner endometrium region, and I is the total intensity in the peri-endometrial region.

Drug and hormone treatment

Levonorgestrel (prescribed from Bundang CHA Medical Center) was diluted to four different concentrations (10, 100, 1000, and 10 000 ng/ml) with EGM-2 and introduced into the media reservoir. The drug was dissolved in DMSO at a concentration of 3 mg/mL as a stock solution. Oestradiol (E2; E8875, Sigma, St. Louis, MO, USA) and progesterone (P4; P8783, Sigma) were diluted into 1 μM and 0.1 μM into EGM-2 media, respectively.

Fluorescent labelling of live and dead cells

Cell viability was assessed using a live/dead viability/cytotoxicity assay (L3224, Invitrogen, Carlsbad, CA, USA). After aspiration of all four media reservoirs of each device, 150 μl of staining solution prepared from 5 ml of EGM-2, 10 μl of ethidium homodimer-1 (Etdh-1, detecting dead cells; Invitrogen), 2.5 μl of Calcein-AM (detecting live cells; Invitrogen), and 5 μl of Hoechst (detecting nuclei; Molecular Probes, Eugene, OR, USA) was pipetted into the media reservoirs. The devices were then incubated at 37°C in 5% CO_2 for 45 min. Fluorescence images were obtained using a confocal microscope (Nikon Ti2-E inverted microscope).

Quantitative PCR-based analysis of mRNA expression

SYBR Green with low ROX (Enzynomics, Daejeon, Korea) assay were used to quantitate angiogenesis and decidualisation-related genes in ESFs treated with E2, E2+P4 and control samples. Total RNA, extracted using TRIzol reagent (Ambion, Life Technologies Corporation, Carlsbad, CA, USA), at 1 μg was converted to cDNA using SuperScript™ IV (GIBCO, Carlsbad, CA, USA). Using a 1/10 volume of cDNA, gene expression was quantitatively analysed. Amplifications were performed using a CFX ConnectTM Real-Time PCR Detection System (Bio-Rad, Hercules, CA, USA). A DNA melting curve was used to confirm the presence of a single PCR product in

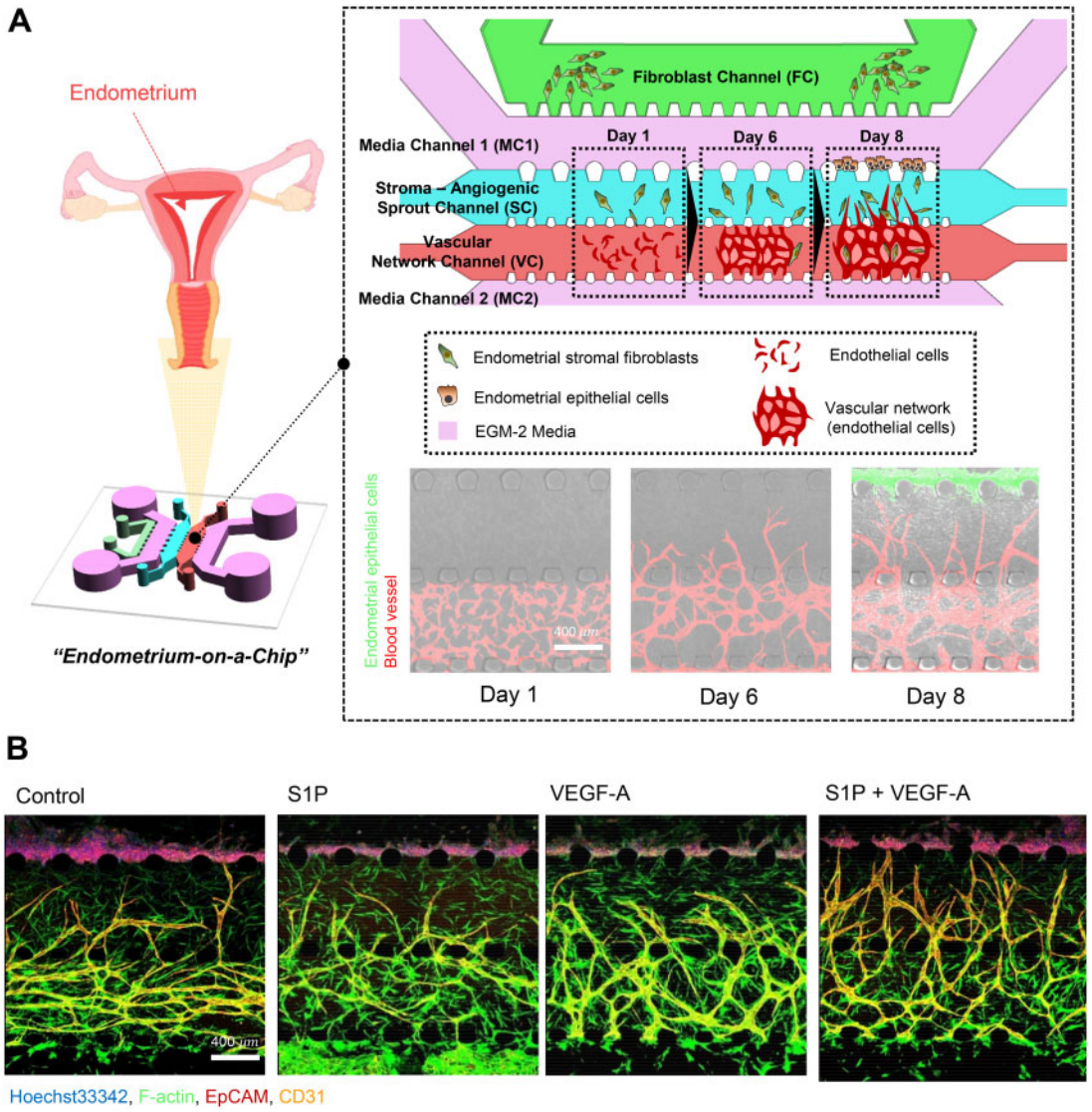

Figure 1. Microfluidic device to reconstitute 3D vascularised endometrial microenvironment. (**A**) Schematic overview and confocal images to mimic natural endometrial microenvironment using a microfluidic 3D tri-culture model, endometrial stromal fibroblasts, endometrial epithelial cells and endothelial cells. Confocal image shows natural endometrial sprouting morphogenesis from the pre-formed blood vessel network. Scale bar, 400 μm. (**B**) Representative confocal images show different angiogenic sprouts response under S1P and VEGF-A. Scale bar, 400 μm.

each assay. Real-time PCR results for decidualisation-related genes were normalised to β-actin mRNA expression and analysed using the ordinary one-way ANOVA analysis with Dunnett's multiple comparison tests. The primer sequence pairs used for these analyses are listed in Supplementary Table SI. The amplification process consisted of 40 cycles: denaturation at 95°C for 10 min, annealing at 58–60°C for 1 min and extension at 72°C for 1 min.

Statistical analysis

Statistical analyses were performed using Prism 6 (GraphPad Software Inc., La Jolla, CA, USA). Comparison groups were analysed using the Student's *t*-test for parametric distributions. For multiple comparisons, the ordinary one-way ANOVA was performed using Dunnett's multiple comparison test. Significance was considered at $P < 0.05$ ($P < 0.05$(*), $P < 0.01$(**), $P < 0.001$(***) and $P < 0.0001$(****)).

Results

Microfluidic device to reconstitute vascularised endometrial microenvironment in a 3D extracellular matrix

Using a microfluidic device (Fig. 1A and Supplementary Fig. S1), we examined the vasculo-angiogenic formation of the microvascular network

depending on different loading patterns of ESFs (Supplementary Fig. S2A). We found that vasculogenic morphogenesis of ECs was dependent on the co-culture with ESFs, because ECs without co-cultured ESFs failed to form interconnected networks (Supplementary Fig. S2B). When ESFs were loaded in the SC, in response to the factors secreted from stromal fibroblasts, vasculogenic morphogenesis of ECs was dramatically increased compared to that in the control ECs (Supplementary Fig. S2C and D). To induce directional angiogenesis, we introduced ESFs in both the SC and FC. Both network formation and angiogenic sprouts were significantly increased compared to the SC patterning only and the control ECs (Supplementary Fig. S2C and D). Culturing ECs without ipsilateral seeding of ESFs (FC) failed to induce robust angiogenic sprout formation, indicating that angiogenic sprouting requires an appropriate directional gradient of pro-angiogenic factors secreted by ESFs. We, therefore, seeded both the SC and FC to mimic the endometrial microenvironment in which the angiogenesis occurs actively. It has been reported that fibroblasts serve as a main source of pro-angiogenic factors (Presta *et al.*, 2005), and that EC morphogenesis is dramatically induced in various 3D model systems (Jeon *et al.*, 2015; Kim *et al.*, 2016). To address whether our model is well suited to assess the effect of pro-angiogenic signalling cues on the growth and morphological changes in the blood vessels of the endometrium, we applied sphingosine 1-phosphate (S1P; 1 μM) and/or vascular endothelial growth factor A (VEGF-A; 50 ng/ml) to the cell culture medium. Angiogenic activity was markedly increased by the treatment with VEGF-A or S1P, displaying higher levels of angiogenic sprouting than in non-treated group, and was synergistically increased with a combined treatment of VEGF-A and S1P (Fig. 1B).

Recapitulation of the uterine cycle within the microengineered endometrium-on-a-chip

To mimic the endometrial physiology during the proliferative and secretory phases of the menstrual cycle in our microengineered endometrium-on-a-chip (MVEOC), we introduced oestradiol (E2) and progesterone (P4) into the culture medium. Proliferative and secretory phases were mimicked by treatment with E2 (Days 8–12; 1 μM) and E2+P4 (Days 8–12; E2: 0.1 μM, P4: 0.1 μM) to the MCs (Fig. 2A and B). ESFs and ECs were loaded into appropriate channels on Day 1, and subsequently the endometrial epithelial layer was established by plating EECs on the side of the SC on Day 8 (Fig. 2B and C). After 4 days of culture, differences in the thickness of the epithelial layer of each group were measured. Both E2-treated and E2+P4-treated groups showed prominently increased thickness in the epithelial layer compared to the control (Fig. 2D and E). Notably, E2 treatment induced higher levels of elevation in epithelial thickness than the E2+P4 combinatorial treatment (Fig. 2E), which is one of the key features of uterine physiology during the E2-dominant proliferative phase (Wang and Dey, 2006). Morphologically, compared to media control, both E2- and E2+P4-treated conditions were characterised by the transformation of elongated ESFs, which displayed strong F-actin expression and significantly increased the F-actin stained surface area compared to the non-treated control (Fig. 3A–C). Furthermore, qRT-PCR analyses revealed that both E2 and the E2+P4 combined treatment significantly increased the mRNA expression of insulin-like growth factor-binding protein 1 (IGFBP1), a well-known marker of decidualisation (Matsumoto *et al.*, 2008; Garrido-Gomez *et al.*, 2017), compared to the control (Supplementary Fig. S3A). We next evaluated the morphological changes in the vasculature in response to E2 or E2+P4 by demonstrating the status of angiogenic sprouts in the SC and vasculogenesis in the VC (Fig. 3D). Within the VC, non-treated and E2-treated conditions showed comparatively evenly distributed in honeycomb-like blood vessel networks. However, a tendency to partially fuse and become interconnected was displayed in E2+P4-treated condition compared to the non-treated or E2-treated conditions (Fig. 3D). Our findings were validated by quantification of angiogenic sprout area in the SC and blood vessel network formation area in the VC, demonstrating significantly decreased blood vessel areas in both the SC and the VC in E2+P4-treated group compared to the E2-treated or control groups (Fig. 3E and F), which is consistent with the expression plot profile for CD31, an endothelial cell marker (Fig. 3G). Results of qRT-PCR analysis showed that E2- and E2+P4-treated ESFs showed significantly increased VEGF-A, which is a well-studied angiogenesis marker (Supplementary Fig. S3B), suggesting that ESFs faithfully recapitulate angiogenic molecular alterations in the MVEOC in response to hormone stimulation.

Probing the effect of levonorgestrel within microengineered endometrium on a chip

The physiological endometrial features observed in our microengineered model system have led us to explore whether our endometrium model on a chip could be used to evaluate the effect of drugs targeting the endometrium, such as the emergency contraception drug, levonorgestrel. Levonorgestrel is a progestin hormone used as an emergency contraceptive, as it causes shedding of the lining of the uterus to prevent the attachment of an embryo (Kahlenborn *et al.*, 2015). The MVEOC was exposed to levonorgestrel for 24 h on Day 11 of culture (Fig. 4A). As the dosage of levonorgestrel was increased, the surface area of propidium iodide staining, indicating dead cells, was correspondingly elevated in both the epithelium and stromal layer in our model (Fig. 4B–D). Subsequently, the blood vessel regression index, the ratio of blood vessel regression which is defined as the final vascular network area divided by the initial vascular network area, was significantly decreased with increasing levonorgestrel doses at 48 h of treatment (Fig. 4E–H).

In the field of drug delivery, the quantitative measurements of drug delivery and monitoring of the local drug delivery sites are crucial for enhancing drug delivery efficacy with controlled safety and toxicity issues (Shi et al., 2010; Jain *et al.*, 2015; Ahn *et al.*, 2018). Thus, appropriate model systems for testing the efficacy of drug delivery are essential. This led us to assess the rates of transmission of levonorgestrel by measuring the permeability of the endometrium in our model. We first compared the thickness and permeability coefficient of the epithelial layer of the co-culture model (EECs–ECs) to those of the tri-culture model (EECs–ESFs–ECs) (Supplementary Fig. S4A). Prior to the measurement, each chip's reservoir was emptied and filled with a solution containing green fluorescent dye to visualise drug transmission efficacy to the endometrium. The tri-culture model showed lower levels of epithelial cell thickness than in the co-culture model with a measurable permeability coefficient (mean: 2.32×10^{-5} cm/s) (Supplementary Fig. S4B and C). However, in the EECs–ECs co-culture system, we were unable to measure the permeability coefficient of the epithelial layer due to overly proliferated and tightly packed EECs (Supplementary Fig. S4D and Supplementary Videos S1 and S2), indicating the significance of the presence of ESFs in maintaining the

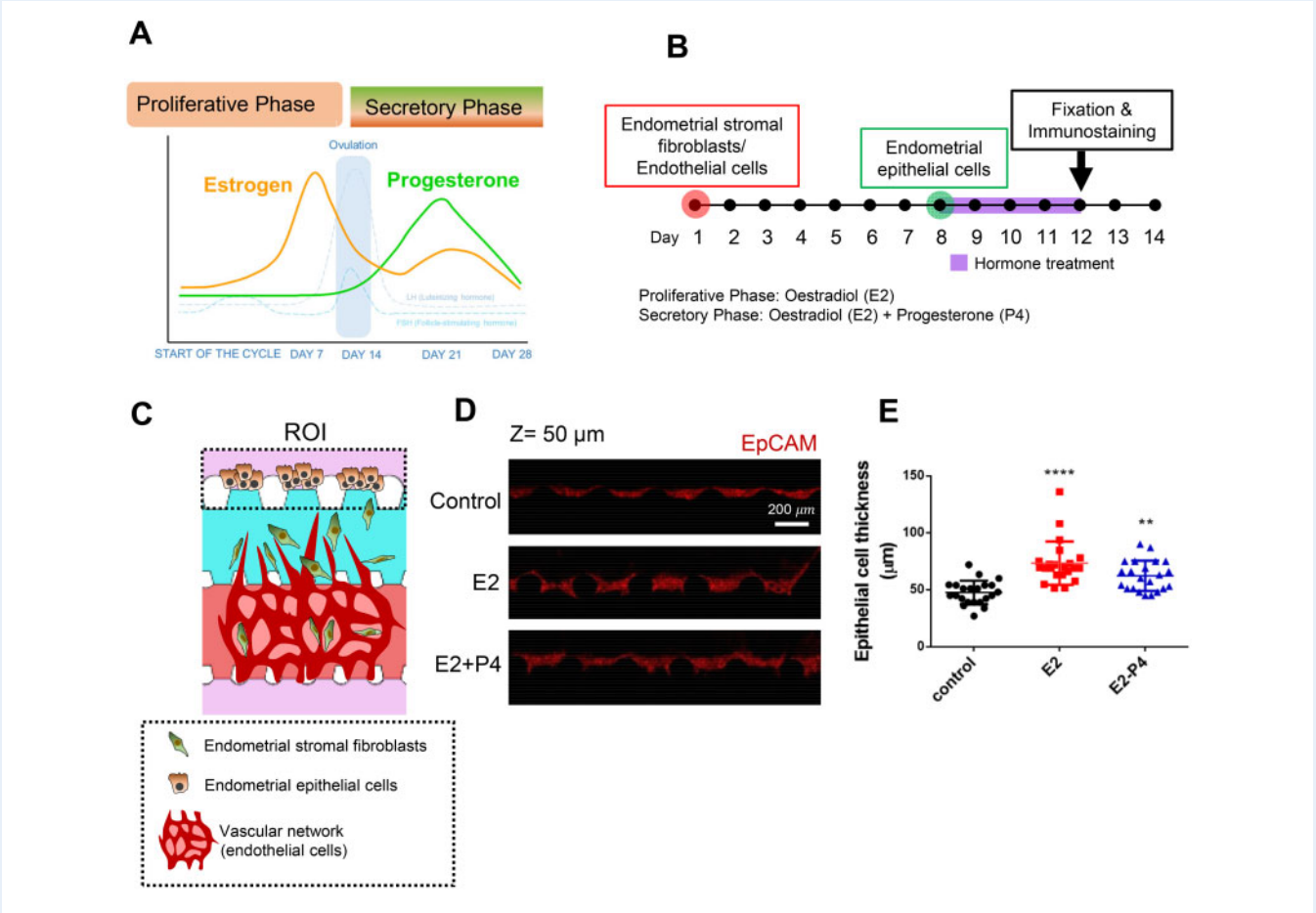

Figure 2. Endometrial epithelial cell responses under proliferative and secretory phase conditions. (**A**) Schematic of the female menstrual cycle showing contribution of the different hormones (oestrogen (E2) and progesterone (P4)). (**B**) Schematic of the experimental process. (**C**) Schematic illustration shows endometrial epithelial cell growth within microfluidic platform. (**D**) Representative confocal microscopic images of endometrial epithelial cells. Scale bar, 200 µm. (**E**) Quantification of endometrial epithelial cell thickness difference in response to E2 and E2+P4 treatment. One-way ANOVA, plotted as mean ± SEM; ** $P < 0.01$, **** $P < 0.0001$.

appropriate function of endometrial permeability. In addition, this was validated by measuring the barrier function of MVEOC using two different molecular weights of FITC-dextrans (10 kDa and 0 kDa). As expected, the permeability coefficient was increased with lower molecular weight FITC-dextran application, displaying an approximately 3-fold increase with 10 kDa FITC-dextran compared to that with 70 kDa FITC-dextran (Supplementary Fig. S4E). Subsequently, we quantified the rates of endometrial permeability in response to levonorgestrel treatment in our model system using 70 kDa FITC-dextran application following 48 h of levonorgestrel treatment (10 000 ng/ml) (Fig. 5A). The permeability coefficient of the levonorgestrel-treated group was 25-fold higher than that of the non-treated group (Fig. 5B and C and Supplementary Video S3).

Proof of concept of 3D microengineered implantation model

The fundamental role of the uterus is to enable an embryo to implant and develop into a foetus (Diedrich et al., 2007). Due to the inaccessibility and the lack of a standard *in-vitro* model system to examine the pre- and peri-implantation phases of pregnancy in the human endometrium, it has not been possible to fully understand the process of embryo implantation at the cellular and molecular levels. Therefore, we further investigated whether physiological aspects of the embryo implantation process could be recapitulated in our model system. Here, we used ligand-conjugated embryo-sized microbeads as a replacement for mouse embryos, as previously suggested (Kang *et al.*, 2014, 2015). Embryo-sized microbeads were coated with heparin-binding EGF-like growth factor (HB-EGF) or insulin-like growth factor 1 (IGF-1), which are well-known factors that are secreted from peri-implanting embryos (Spaventi et al., 1990; Hamatani *et al.*, 2004; Kim *et al.*, 2005; Kang *et al.*, 2014). HB-EGF- and IGF-1-coated microbeads were introduced through the a media channel (Fig. 6A and B). Of note, to induce more stable attachment of microbeads in between of microposts, the microfluidic post design was modified to a crown-shaped one (Supplementary Fig. S1). As a consequence, ligand-conjugated microbeads were found to be attached to the boundary of endometrial epithelial layer next to the medial channel but not on the

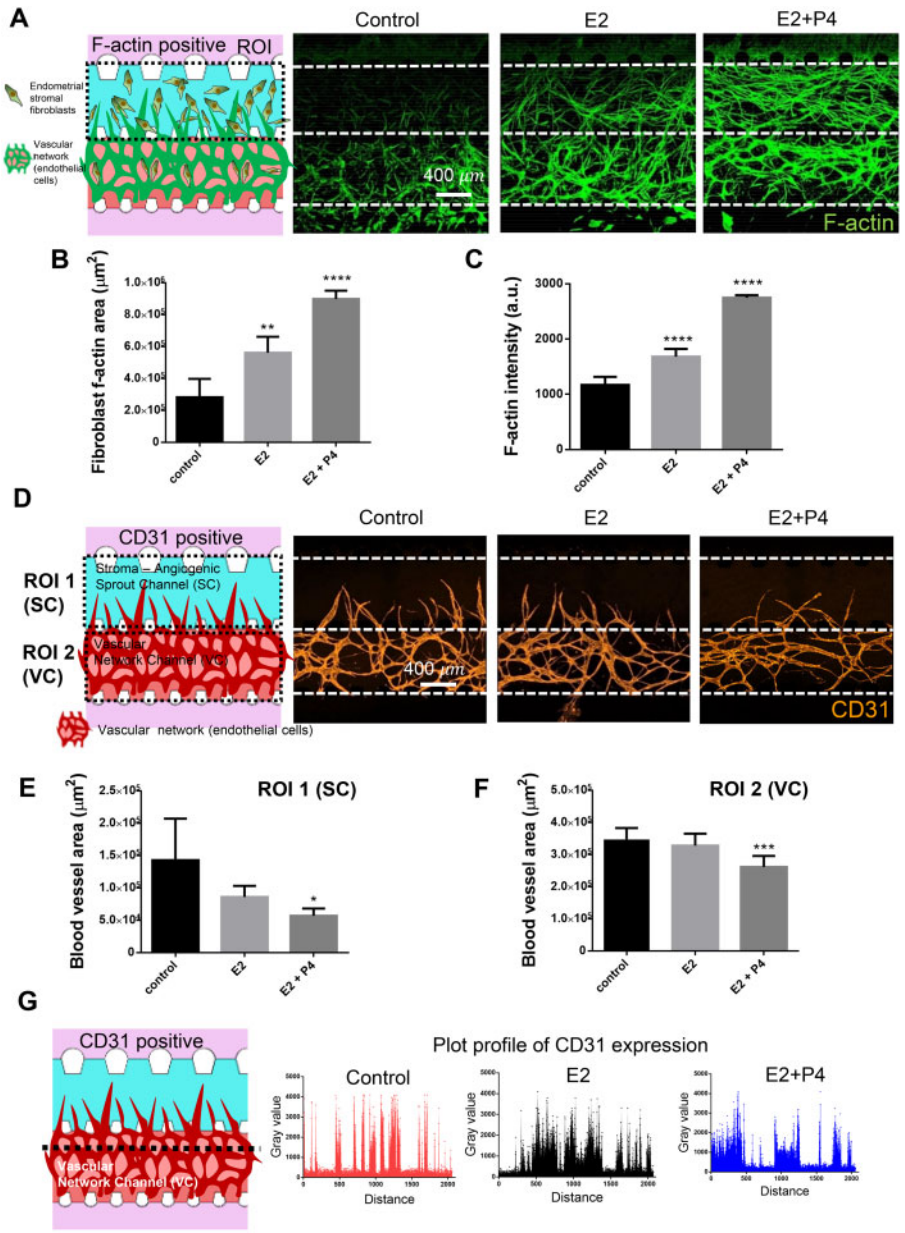

Figure 3. Oestradiol and progesterone response of endometrial stromal fibroblasts and endothelial cells within 3D endometrium on a chip. (**A**) Schematic illustration and representative confocal images of F-actin cytoskeleton of endometrial stromal fibroblasts. Scale bar, 400 μm. (**B**) F-actin cytoskeleton area of endometrial stromal fibroblasts. (**C**) F-actin intensity of endometrial stromal fibroblasts. (**D**) Schematic illustration and representative confocal image of angiogenic sprouts and vascular network. Scale bar, 400 μm. (**E**) Angiogenic sprouts area in stroma-angiogenic sprout channel. (**F**) Vascular network area in vascular network channel. (**G**) CD31-positive plot profile of arbitrary transverse line one-way ANOVA, plotted as mean ± SEM; $*P < 0.05$, $**P < 0.01$, $***P < 0.001$, and $****P < 0.0001$.

PDMS microposts (Fig. 6C). After co-culture for 2 h, the attachment rates of ligand-conjugated microbeads were measured using hydrostatic shear stress induced by a media volume difference of ~100 μl. While ~60% of bovine serum albumin (BSA)-coated microbeads (control group) remained attached, ~85% of beads carrying HB-EGF and IGF-1 were stably attached to the surface of epithelial cells (Fig. 6D), suggesting that our model may be applicable for investigating complex implantation mechanisms that involve various physiological and molecular processes.

Discussion

To provide biologically highly relevant specific testing platforms of the critical reproductive organ, the endometrium, we established a

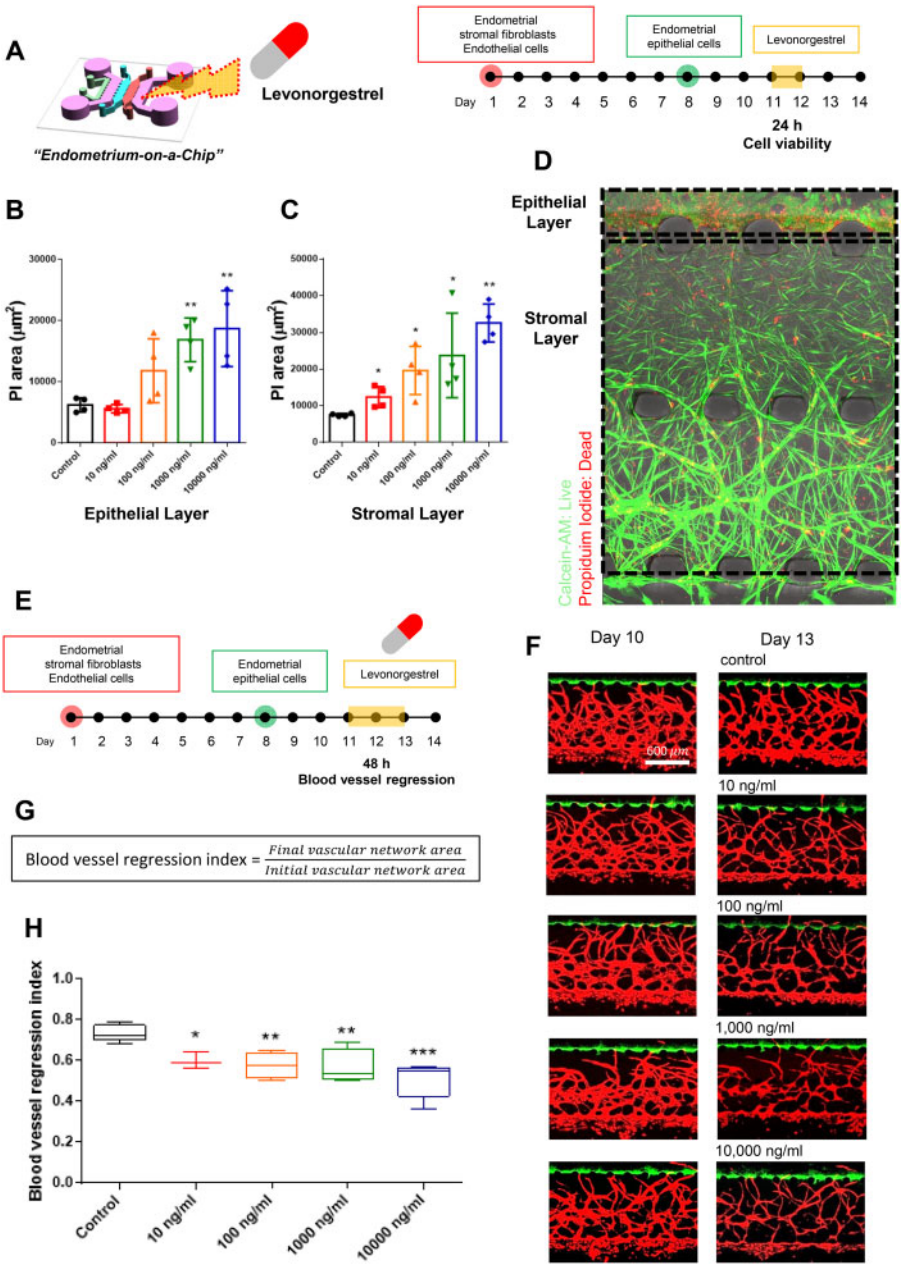

Figure 4. Levonorgestrel response in 3D endometrium-on-a-chip. (**A**) Schematic illustration of levonorgestrel treatment on 3D endometrium-on-a-chip. (**B** and **C**) Propidium iodide area of the epithelium layer and stromal layer, respectively. (**D**) Representative confocal images represent live/dead signals. (**E**) Schematic illustration of levonorgestrel treatment on 3D endometrium-on-a-chip and blood vessel regression monitoring. (**F**) Representative confocal image of angiogenic sprouts and vascular network before levonorgestrel treatment (Day 10) and after levonorgestrel treatment (Day 13). Scale bar, 600 μm. (**G**) Blood vessel regression index was calculated as the ratio of final vascular network area to initial vascular network area. (**H**) Blood vessel regression index in response to different levonorgestrel dosages from 0 to 10 000 ng/ml. One-way ANOVA, plotted as mean ± SEM; * $P < 0.05$, ** $P < 0.01$, and *** $P < 0.001$.

MVEOC, which consists of three distinct layers; epithelium, stroma and blood vessels. In our representative model, we demonstrated that human blood endothelial cells co-cultured with ESFs, which greatly stimulate the morphogenesis of endothelial cells both during vasculogenic and angiogenic processes, spontaneously organise into an interconnected microvascular network and then further expand to adjacent (endometrial fibroblast region) avascular regions in a manner of neovessel sprouting, which is physiologically relevant to endometrial vessel formation near the uterine cavity (Fig. 1).

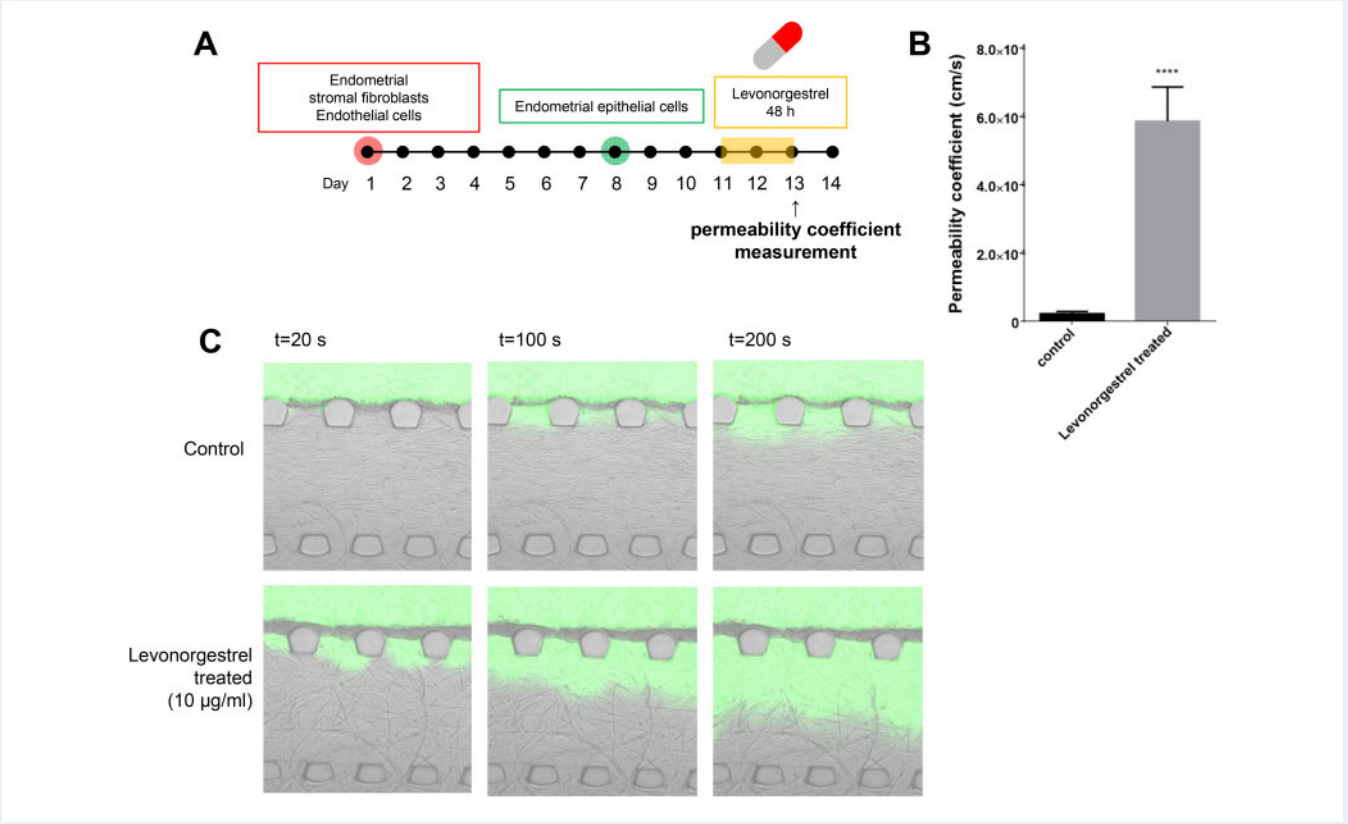

Figure 5. Endometrial permeability measurement in response to levonorgestrel treatment. (**A**) Schematic of the experimental process of permeability measurement with levonorgestrel treatment. Endometrial permeability was measured after 48 h treatment of levonorgestrel. (**B**) The levonorgestrel-treated condition showed significantly higher permeability than that of the control. (**C**) Time series fluorescence micrographs were captured and analysed for endometrial permeability. Non-paired Student's *t*-test, plotted as mean ± SD; **** $P < 0.0001$.

The human endometrium undergoes cyclical development in the absence of a pregnancy. A crucial part of this process is the growth of new blood vessels required to furnish the expanding endometrium. Research on endometrial function has focused not only on the steroidal regulation of epithelial and stromal cell proliferation and regression, but also on proper cyclical angiogenesis for normal reproductive processes and placental development (Reynolds *et al.*, 2005). Throughout pregnancy, various pro-angiogenic factors, including VEGF-A and S1P, are produced in the uterus by the decidua, placenta and endometrium, stimulating new blood vessel growth (Herr *et al.*, 2003; Duran *et al.*, 2018). We demonstrated that our MVEOC faithfully recapitulates endometrial angiogenesis *in vivo* in response to VEGF-A and S1P. Indeed, the demand for angiogenesis differs spatially and temporally in the endometrium. Angiogenesis occurs in the basalis layer during menstruation and in the functionalis during the proliferative and secretory phases. Unlike most of *in-vitro* models of the endometrium, by virtue of microfluidic-based 3D cell culture, the *in vivo* like endometrial microenvironment was recapitulated in a 3D extracellular matrix in a spatiotemporal manner.

To recapitulate the proliferative and secretory phases of the menstrual cycle, we introduced E2 to mimic the proliferative phase and E2 and P4 for the secretory phase and quantified the physiological responses of each distinct epithelium, stroma and blood vessel layers. Notably, the E2+P4-treated group showed more dramatic changes in the ESFs than the E2-treated group. Actin, which is concentrated in the cortex of decidual cells, most often in a filamentous form (i.e. F-actin), regulates the intracellular reorganisation which results in shape changes (Ihnatovych *et al.*, 2009). Indeed, decidualisation is critical for the successful establishment and maintenance of pregnancy in humans. It describes a complex cell transformation which requires morphological and functional changes in the cell structure and involves the reorganisation of the cytoskeleton. Proper cytoskeletal organisation and function depend on cytoskeletal dynamics which is the interaction between actin and myosin. The proliferative and secretory phases are marked by the active growth of epithelial and stromal cells. The increased thickness of the epithelium and then the increased F-actin area indicate that our model can recapitulate key characteristics of the *in-vivo* endometrial environment.

Vasculogenesis and angiogenesis are crucial during the menstrual cycle and during implantation. These processes are also related to the development of the fetal and placental vasculatures. By the virtue of our platform design, we could examine the sequential progress of vasculogenic formation in the VC and its subsequent expansion into the adjacent SC. In response to the factors secreted from stromal fibroblasts in the channel SC and FC, in which multiple signalling cues are orchestrated, ECs in the fibrin matrix initiated the formation of

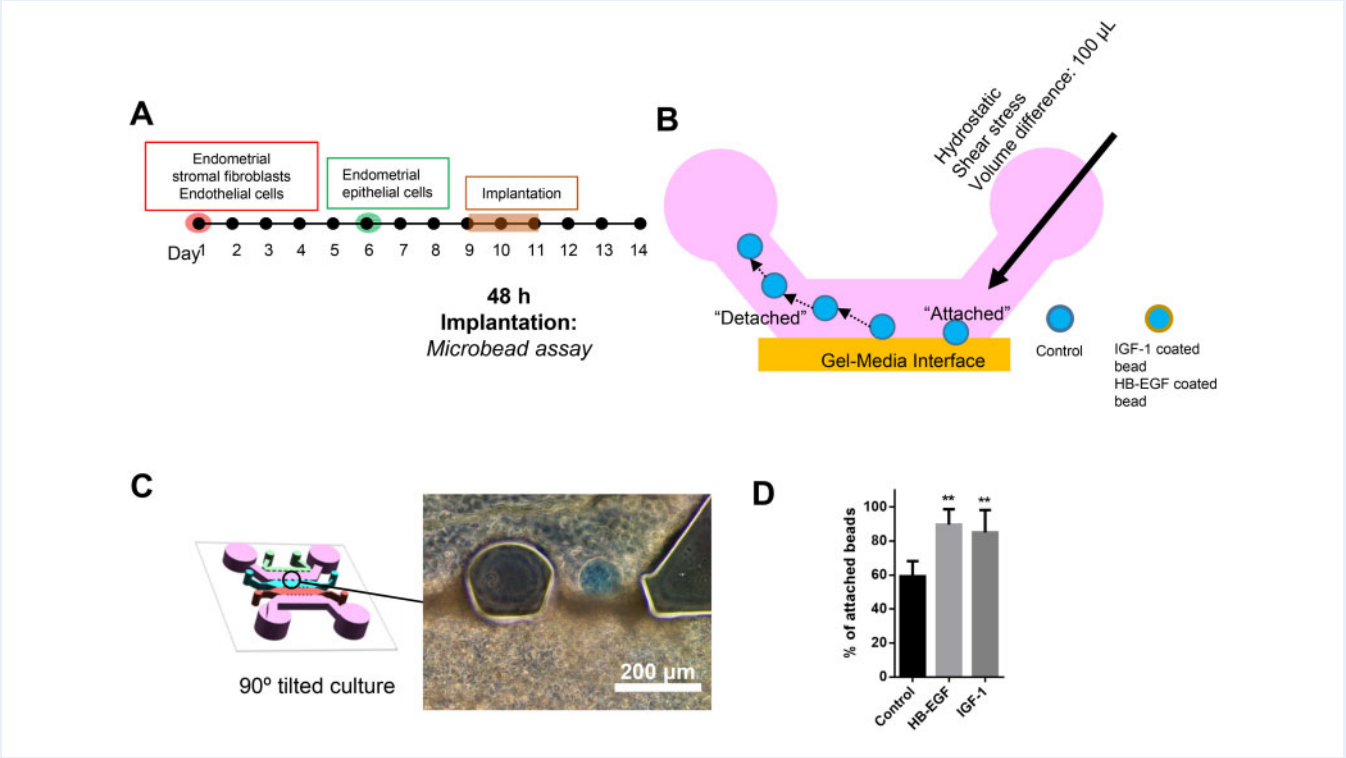

Figure 6. 3D microengineered implantation model. (**A** and **B**) Schematic of the experimental process of testing the 3D microengineered implantation model. (**C**) Bright field image of stably attached protein-coated microbeads. Scale bar: 200 µm. (**D**) Graph shows that beads carrying HB-EGF and IGF-1 exhibited significantly higher attachment than BSA-coated microbeads. One-way ANOVA, plotted as mean ± SEM; ** $P < 0.01$.

intracellular vacuoles and extended protrusions, which progressively developed into interconnected, honeycomb-like vascular networks. The formation of angiogenic sprouts from the vascular network was also observed. These angiogenic sprouts exhibited a complex interconnected and bifurcated architecture similar to that found in native vasculature. Using our platform, we observed morphological changes in the vasculature in response to E2 (proliferative phase) and E2+P4 (secretory phase) (Fig. 3D). During the proliferative and secretory phases, active endometrial angiogenic activity was observed *in vivo*. However, in our current system, there was no statistical difference in the E2- and E2+P4-treated groups compared to the control. Endometrial angiogenesis encompasses an intricate coupled angiogenesis mechanism. Although endometrial angiogenesis is under the hormonal control of E2 and P4, these hormones act indirectly via many other angiogenesis regulators. The complex processes of angiogenesis in the endometrium are tightly regulated by angiogenic and anti-angiogenic factors in a system that can probably be turned on and off within a short time (Gargett and Rogers, 2001l Smith, 2001; Okada *et al.*, 2018). Several angiogenic factors that play important roles in physiological angiogenesis have been identified in the human endometrium. Consistently, increased VEGF-A with E2 and E2+P4 in ESFs (Supplementary Fig. 3B) may recapitulate maturation of uterine blood vessels during the secretory phase, which is a key feature that is critical for the formation of the maternal part of the placenta and decidua that supply oxygen and nutrients to the fetus (Gambino *et al.*, 2002).

Levonorgestrel, the first progestin-only type of emergency contraception, has garnered considerable attention as it is the most widely used emergency contraception worldwide (Cleland *et al.*, 2014; Kahlenborn *et al.*, 2015). As the levonorgestrel dosage increased, the dead cell signal was increased in both the epithelial and stromal layers within our platform (Fig. 4B–D), which is consistent with previous reports showing a significant increase in apoptosis-positive nuclei in the endometrium after insertion of a levonorgestrel-releasing intrauterine system (Maruo *et al.*, 2001). Here, we determined the blood vessel regression index and a significant decrease was observed with increasing levonorgestrel doses (Fig. 4G). In the majority of cases, levonorgestrel reduces the endometrial thickness, as evidenced by ultrasonography, and increased vascular resistance in the uterine artery with decreased uterine blood flow and a marked reduction in subendometrial blood flow (Zalel *et al.*, 2002; Jimenez *et al.*, 2008). These results demonstrate that our physiologically relevant model provides a quantitative evaluation of pharmacological agents targeting the endometrium and precise reflection of phenotypic changes associated with the mechanistic action of the agents. Many intrauterine drug delivery products have been developed with improved methods for the prevention and treatment of gynaecological conditions. In this study, we evaluated the endometrial permeability in response to levonorgestrel treatment. The permeability coefficient of the levonorgestrel-treated group was significantly higher than that of the non-treated group, indicating that the levonorgestrel directly increased endometrial permeability (Fig. 5 and Supplementary Video S3). After levonorgestrel application, the

endometrium loses structural integrity and becomes leaky, possibly displaying a haemorrhage-like condition in the stromal layer of the endometrium. Our findings strongly suggest that our MVEOC can provide a tool for high-throughput drug screening, *in-vitro* simulation of the *in-vivo* endometrial environment, and improvements in potential drug candidate screening efficiency.

Implantation is the stage of pregnancy at which the embryo adheres to the wall of the uterus. Owing to the inaccessibility of the human implantation site *in vivo*, many efforts to collect tissues from the sites of implanted embryos have mostly failed. We and others (Dominguez *et al.*, 2010) have established various types of *in-vitro* models for embryo implantation to overcome the difficulties of *in-vivo* studies in humans and differences among species. However, none of these have been reproducible and have allowed mimicking of the endometrial vasculo-angiogenesis, which plays a crucial role during the embryo implantation. In our representative endometrial model, we used a well-differentiated Ishikawa cell line in which the cell surface and steroid hormone receptor phenotype have prominent similarities to normal epithelial cells (Aplin, 1995; Hannan *et al.*, 2010). To reflect the complex but organised endometrial stromal microenvironment, the CRL-4003 cell line and HUVECs were used. Moreover, HB-EGF- and IGF-1-coated beads were used to mimic embryos secreting HB-EGF and IGF-1, as previously suggested (Kang *et al.*, 2014). In this study, we show proof of concept for an *in-vitro* embryo implantation model which could potentially identify the identification of molecular pathways involved in the process of embryo implantation.

Compared to conventional macroscale *in-vitro* culture systems, microfluidic-based organ-on-a-chip technology provides physiologically relevant organ-specific testing platforms capable of mimicking the *in-vivo* microenvironment. Our model is the first organ-on-a-chip that closely recapitulates the endometrial microenvironment using human endometrial epithelial cells, stromal fibroblasts and endothelial cells. Combining microfabrication techniques with modern 3D tissue engineering, MVEOC provides a new *in-vitro* approach to drug screening and drug discovery that mimics the complex physiological features of the human endometrium for addressing critical challenges and unsolved problems in female diseases such as endometriosis, uterine cancer and female infertility.

Supplementary data

Supplementary data are available at *Human Reproduction* online.

Data availability

The data underlying this research article can be made available upon reasonable request to the corresponding author.

Authors' roles

Y.J.K. and J.A. planned the studies and conducted the analysis and interpretation of all experiments; J.A., M.J.Y., S.H.H., H.C. and D.L. conducted the experiments; H.S.K., J.E.K., J.L., S.O. and N.L.J. contributed to critical discussions; and J.A. and Y.J.K. wrote the manuscript.

Funding

This work is supported by funding from the National Research Foundation of Korea (NRF) grant funded by the Korea government (MSIT) to Y.J.K. (No. 2018R1C1B6003), to J.A. (No. 2020R1I1A1A01074136), and to H.S.K. (No. 2020R1C1C100787212).

Conflict of interest

The authors declare that there is no conflict of interests.

References

Ahn J, Cho CS, Cho SW, Kang JH, Kim SY, Min DH, Song JM, Park TE, Jeon NL. Investigation on vascular cytotoxicity and extravascular transport of cationic polymer nanoparticles using perfusable 3D microvessel model. *Acta Biomater* 2018;**76**:154–163.

Ahn J, Ko J, Lee S, Yu J, Kim Y, Jeon NL. Microfluidics in nanoparticle drug delivery; from synthesis to pre-clinical screening. *Adv Drug Deliv Rev* 2018;**128**:29–53.

Aplin JD. Molecular and cellular aspects of peri-implantation processes, Boston, Massachusetts 15–18 July 1994. *Placenta* 1995;**16**:109–111.

Blundell C, Tess ER, Schanzer AS, Coutifaris C, Su EJ, Parry S, Huh D. A microphysiological model of the human placental barrier. *Lab Chip* 2016;**16**:3065–3073.

Brar AK, Frank GR, Kessler CA, Cedars MI, Handwerger S. Progesterone-dependent decidualization of the human endometrium is mediated by cAMP. *Endocrine* 1997;**6**:301–307.

Catalini L, Fedder J. Characteristics of the endometrium in menstruating species: lessons learned from the animal kingdom. *Biol Reprod* 2020;**102**:1160–1169.

Cleland K, Raymond EG, Westley E, Trussell J. Emergency contraception review: evidence-based recommendations for clinicians. *Clin Obstet Gynecol* 2014;**57**:741–750.

Diedrich K, Fauser BC, Devroey P, Griesinger G, Evian Annual Reproduction (EVAR) Workshop Group. The role of the endometrium and embryo in human implantation. *Hum Reprod Update* 2007;**13**:365–377.

Dominguez F, Simon C, Quinonero A, Ramirez MA, Gonzalez-Munoz E, Burghardt H, Cervero A, Martinez S, Pellicer A, Palacin M. *et al.* Human endometrial CD98 is essential for blastocyst adhesion. *PLoS One* 2010;**5**:e13380.

Duran CL, Abbey CA, Bayless KJ. Establishment of a three-dimensional model to study human uterine angiogenesis. *Mol Hum Reprod* 2018;**24**:74–93.

Gambino LS, Wreford NG, Bertram JF, Dockery P, Lederman F, Rogers PA. Angiogenesis occurs by vessel elongation in proliferative phase human endometrium. *Hum Reprod* 2002;**17**:1199–1206.

Gargett CE, Rogers PA. Human endometrial angiogenesis. *Reproduction* 2001;**121**:181–186.

Garrido-Gomez T, Dominguez F, Quinonero A, Diaz-Gimeno P, Kapidzic M, Gormley M, Ona K, Padilla-Iserte P, McMaster M, Genbacev O. *et al.* Defective decidualization during and after

severe preeclampsia reveals a possible maternal contribution to the etiology. *Proc Natl Acad Sci U S A* 2017;**114**:E8468–E8477.

Gnecco JS, Ding T, Smith C, Lu J, Bruner-Tran KL, Osteen KG. Hemodynamic forces enhance decidualization via endothelial-derived prostaglandin E2 and prostacyclin in a microfluidic model of the human endometrium. *Hum Reprod* 2019;**34**:702–714.

Hamatani T, Carter MG, Sharov AA, Ko MS. Dynamics of global gene expression changes during mouse preimplantation development. *Dev Cell* 2004;**6**:117–131.

Hannan NJ, Paiva P, Dimitriadis E, Salamonsen LA. Models for study of human embryo implantation: choice of cell lines? *Biol Reprod* 2010;**82**:235–245.

Herr F, Liang OD, Herrero J, Lang U, Preissner KT, Han VK, Zygmunt M. Possible angiogenic roles of insulin-like growth factor II and its receptors in uterine vascular adaptation to pregnancy. *J Clin Endocrinol Metab* 2003;**88**:4811–4817.

Hibaoui Y, Feki A. Organoid models of human endometrial development and disease. *Front Cell Dev Biol* 2020;**8**:84.

Ihnatovych I, Livak M, Reed J, de Lanerolle P, Strakova Z. Manipulating actin dynamics affects human in vitro decidualization. *Biol Reprod* 2009;**81**:222–230.

Jain K, Mehra NK, Jain NK. Nanotechnology in drug delivery: safety and toxicity issues. *Curr Pharm Des* 2015;**21**:4252–4261.

Jeon JS, Bersini S, Gilardi M, Dubini G, Charest JL, Moretti M, Kamm RD. Human 3D vascularized organotypic microfluidic assays to study breast cancer cell extravasation. *Proc Natl Acad Sci U S A* 2015;**112**:214–219.

Jimenez MF, Arbo E, Vetori D, de Freitas FM, Cunha-Filho JS. The effect of the levonorgestrel-releasing intrauterine system and the copper intrauterine device on subendometrial microvascularization and uterine artery blood flow. *Fertil Steril* 2008;**90**:1574–1578.

Kahlenborn C, Peck R, Severs WB. Mechanism of action of levonorgestrel emergency contraception. *Linacre Q* 2015;**82**:18–33.

Kang YJ, Forbes K, Carver J, Aplin JD. The role of the osteopontin-integrin alphavbeta3 interaction at implantation: functional analysis using three different in vitro models. *Hum Reprod* 2014;**29**:739–749.

Kang YJ, Lees M, Matthews LC, Kimber SJ, Forbes K, Aplin JD. MiR-145 suppresses embryo-epithelial juxtacrine communication at implantation by modulating maternal IGF1R. *J Cell Sci* 2015;**128**:804–814.

Kim S, Chung M, Ahn J, Lee S, Jeon NL. Interstitial flow regulates the angiogenic response and phenotype of endothelial cells in a 3D culture model. *Lab Chip* 2016;**16**:4189–4199.

Kim S, Lee GS, Lee SH, Kim HS, Jeong YW, Kim JH, Kang SK, Lee BC, Hwang WS. Embryotropic effect of insulin-like growth factor (IGF)-I and its receptor on development of porcine preimplantation embryos produced by in vitro fertilization and somatic cell nuclear transfer. *Mol Reprod Dev* 2005;**72**:88–97.

Kobayashi A, Behringer RR. Developmental genetics of the female reproductive tract in mammals. *Nat Rev Genet* 2003;**4**:969–980.

Lee JS, Romero R, Han YM, Kim HC, Kim CJ, Hong JS, Huh D. Placenta-on-a-chip: a novel platform to study the biology of the human placenta. *J Matern Fetal Neonatal Med* 2016;**29**:1046–1054.

Lim H, Ma L, Ma WG, Maas RL, Dey SK. Hoxa-10 regulates uterine stromal cell responsiveness to progesterone during implantation and decidualization in the mouse. *Mol Endocrinol* 1999;**13**:1005–1017.

Maruo T, Laoag-Fernandez JB, Pakarinen P, Murakoshi H, Spitz IM, Johansson E. Effects of the levonorgestrel-releasing intrauterine system on proliferation and apoptosis in the endometrium. *Hum Reprod* 2001;**16**:2103–2108.

Matsumoto H, Sakai K, Iwashita M. Insulin-like growth factor binding protein-1 induces decidualization of human endometrial stromal cells via alpha5beta1 integrin. *Mol Hum Reprod* 2008;**14**:485–489.

McGowen MR, Erez O, Romero R, Wildman DE. The evolution of embryo implantation. *Int J Dev Biol* 2014;**58**:155–161.

Okada H, Tsuzuki T, Murata H. Decidualization of the human endometrium. *Reprod Med Biol* 2018;**17**:220–227.

Presta M, Dell'Era P, Mitola S, Moroni E, Ronca R, Rusnati M. Fibroblast growth factor/fibroblast growth factor receptor system in angiogenesis. *Cytokine Growth Factor Rev* 2005;**16**:159–178.

Reed BG, Carr BR, KR Feingold, B Anawalt, A Boyce, G Chrousos, WW de Herder, K Dhatariya, K Dungan, A Grossman, JM Hershman, J. Hofland *et al.* (eds). The normal menstrual cycle and the control of ovulation. In *Endotext*. South Dartmouth, MA: MDText.com, 2000.

Reynolds LP, Borowicz PP, Vonnahme KA, Johnson ML, Grazul-Bilska AT, Redmer DA, Caton JS. Placental angiogenesis in sheep models of compromised pregnancy. *J Physiol* 2005;**565**:43–58.

Roy A, Matzuk MM. Reproductive tract function and dysfunction in women. *Nat Rev Endocrinol* 2011;**7**:517–525.

Shi J, Votruba AR, Farokhzad OC, Langer R. Nanotechnology in drug delivery and tissue engineering: from discovery to applications. *Nano Lett* 2010;**10**:3223–3230.

Smith SK. Regulation of angiogenesis in the endometrium. *Trends Endocrinol Metab* 2001;**12**:147–151.

Spaventi R, Antica M, Pavelic K. Insulin and insulin-like growth factor I (IGF I) in early mouse embryogenesis. *Development* 1990;**108**:491–495.

Taylor E, Gomel V. The uterus and fertility. *Fertil Steril* 2008;**89**:1–16.

Wang H, Dey SK. Roadmap to embryo implantation: clues from mouse models. *Nat Rev Genet* 2006;**7**:185–199.

Xiao S, Coppeta JR, Rogers HB, Isenberg BC, Zhu J, Olalekan SA, McKinnon KE, Dokic D, Rashedi AS, Haisenleder DJ. *et al.* A microfluidic culture model of the human reproductive tract and 28-day menstrual cycle. *Nat Commun* 2017;**8**:14584.

Zalel Y, Shulman A, Lidor A, Achiron R, Mashiach S, Gamzu R. The local progestational effect of the levonorgestrel-releasing intrauterine system: a sonographic and Doppler flow study. *Hum Reprod* 2002;**17**:2878–2880.